DEPARTMENT OF MATERIALS AND CONSTRUCTION

Analysis of Triaxial Test Data on Asphalt Concrete Using Viscoelastic Principles

K. E. SECOR AND C. L. MONISMITH,
Respectively, Assistant Research Engineer and Assistant Professor of Civil Engineering, Institute of Transportation and Traffic Engineering, University of California, Berkeley

• CONSIDERABLE evidence has been obtained in recent years suggesting that the stress versus strain characteristics of the materials comprising the structural section of flexible pavements are time dependent. Inasmuch as the load conditions which may be imposed upon such pavements cover a wide range in time—from the essentially static condition associated with vehicle parking areas to the rapidly applied repeated loads occurring on heavy-duty highways and airfield taxiways—it would seem appropriate to apply the principles of viscoelastic theory in preparing a more rigorous approach to the analysis of these structures. The many as yet unsolved problems posed by increasing traffic demands, both in magnitude and frequency of loading, fortify the argument for such an approach.

Before such an analysis can be developed, however, it is necessary to establish the essential properties of the various materials comprising the pavement. Some research (*1*) indicates that the physical behavior of soils can be expressed in terms of viscoelastic parameters; however, much more information is required to provide suitable data on soil behavior from this standpoint. Considerable evidence has been presented (*2, 3, 4*) illustrating the viscoelastic behavior of asphalts. Some data pointing to similar behavior in asphalt mixtures are also available (*5, 6, 7, 8, 9*). As with soil, however, more information on asphalt concrete is required before the behavior of the structural section can be reliably analyzed from the viscoelastic approach. Hence, this paper presents data which, it is hoped, will add to this required information.

It is believed that the desired viscoelastic properties of asphalt paving mixtures can best be studied by means of the triaxial compression test. Therefore, the test results and related theoretical developments were developed by this means. Actually, two methods of analysis are presented. The first part of the work is concerned with the possibility of eliminating lateral pressure effects through the application of the concept of deviatoric

stress and strain, leaving only temperature and time effects to be evaluated by other means. The second part is concerned with the use of viscoelastic model theory to evaluate the results of four different types of triaxial tests: (a) creep tests, (b) relaxation tests, (c) constant-rate-of-strain tests, and (d) repeated-load tests. The possibility of mathematically relating the results of such measurements within the viscoelastic framework is one of the salient features of this type of analysis and examples of the feasibility of this approach are presented.

MATERIALS

One 85-100 penetration asphalt cement was used in the investigations. Results of standard tests on the material are given in Table 1.

In addition to the standard tests, absolute viscosity measurements by means of the Shell microviscometer (*10*) and the Lantz Zeitfuchs capillary viscometer (ASTM D445-53T,

TABLE 1
IDENTIFICATION TESTS ON ASPHALT

Test	Result
Penetration at 77°F, 100 gm, 5 sec	96
Penetration at 39.2°F, 200 gm, 60 sec	24
Penetration ratio	25
Flash point, Pensky-Martens, °F	445
Viscosity at 275°F, SSF	138
Heptane-xylene equivalent	20/25
Softening point, ring and ball, °F	110
Thin film oven test, 325°F, 5 hr:	
Percent weight loss	0.51
Percent penetration retained	53
Ductility of residue	100+

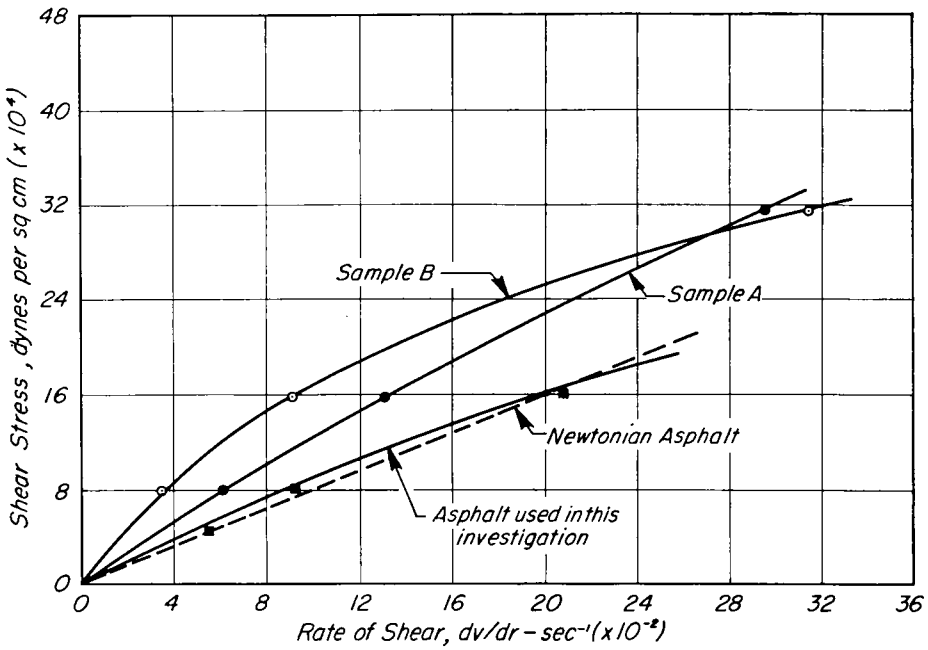

Sample A --- 85-100 Pen. asphalt, Calif. Division of Highways Spec., 1960
Sample B --- 85-100 Pen. asphalt, Air Blown.
Newtonian Asphalt --- 85-100 Pen. asphalt, Calif. Division of Highways Spec., 1954

Figure 1. Shear stress *vs* rate of shear relationships at 77 F.

Appendix G) were performed on the asphalt. Figure 1 shows the shear stress-rate of shear relationship for this material at 77 F. Also shown, for purposes of comparison, are similar plots for the results of tests performed on two asphalts used in previous research at the University of California (*8, 9, 11, 12*) and on a material conforming to the 1954 Standard Specifications (*13*) of the California Division of Highways. It can be seen that the asphalt used in the present study approaches Newtonian behavior at this temperature. Figure 2 shows the variation of absolute viscosity with temperature at a shear rate of 5×10^{-2} sec^{-1} for this material, as well as for the other asphalts cited for comparison. A point worth noting, because it might have considerable bearing on the viscoelastic constants of any paving mixtures prepared with these four asphalts, is the fact that, although all are classified as 85-100 penetration asphalt cements, their absolute viscosity characteristics vary considerably with temperature and with rate of shear.

One aggregate, a crushed granite from Watsonville, Calif., with a uniform specific gravity of 2.92 (ASTM C127-42, ASTM C128-42) was used. This material has been used in other laboratory investigations at the University of California (*11, 12*) and has

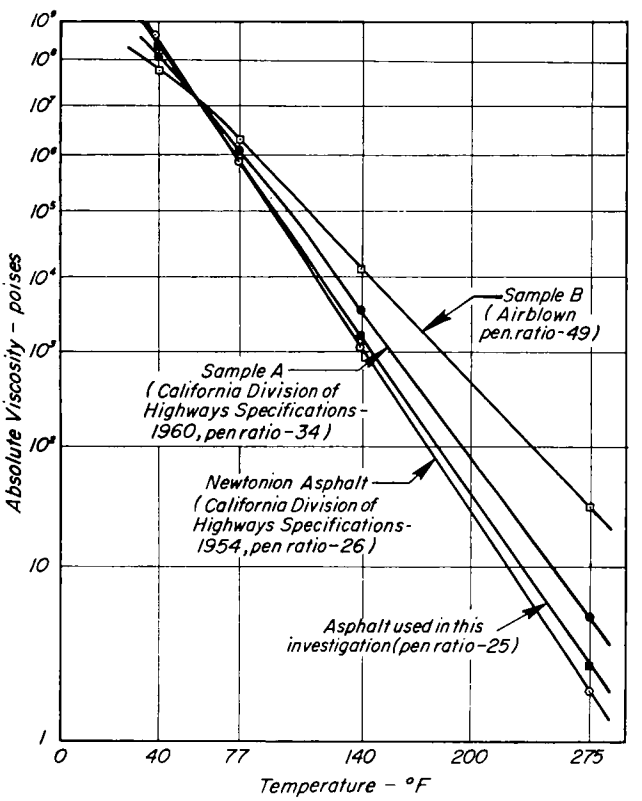

Figure 2. Temperature *vs* viscosity relationships for asphalt cements (log log (viscosity constant) *vs* log absolute temperature) — viscosity determined at shear rate of 5×10^{-2} sec^{-1}.

an excellent service record in pavements throughout that State. One dense gradation of the aggregate was used (Fig. 3). To insure that all specimens would have the same proportions, the material was separated into individual size fractions by screening and then recombined into separate batches of the amount required to prepare single samples. A ⅜-in. maximum size was adopted, as this was judged to be the limit imposed by the dimensions of the triaxial specimens (*12*).

PREPARATIONS OF TEST SPECIMENS

The blending, proportioning, mixing, and curing operations for the specimens were carefully controlled. Mixing of the asphalt and aggregate was performed at 250 F in a mechanically-driven, vertical-bowl mixer for a period of 5 min. After mixing, each specimen was cured for 24 hr at 140 F.

Following curing, each mixture was compacted at 250 F into a cylindrical specimen 2.78 in. in diameter and approximately 6.40 in. in height by means of kneading compaction using the "low-cost kneading compactor" (*14*). Uniform density throughout the height of each specimen was obtained by compacting the sample in 5 layers with 25 tamps per layer, wth an additional 25 tamps on the surface, at a 500-psi compaction pressure. After compaction, a 500-psi leveling load was applied to the surface of each specimen.

One asphalt constant of 6 percent (by weight of aggregate) was selected for the tests. This asphalt content approximates the design value for the type and gradation of aggregate used based on the California design procedure for asphalt paving mixtures.

Prior to testing the specific gravity of each specimen was determined by water displacement and a unit weight approximating 150 pcf was obtained for all specimens.

TEST PROCEDURES

All tests were performed in triaxial cells, as shown schematically in Figure 4, which also shows the water bath used to obtain constant-temperature conditions (within ± 0.5 F) during testing. Any desired temperature between about 35 F and 140

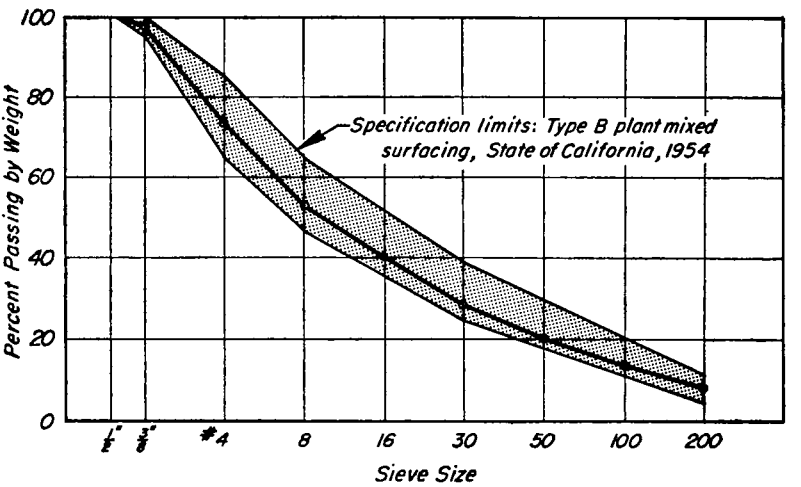

Figure 3. Grading curve, Watsonville aggregate.

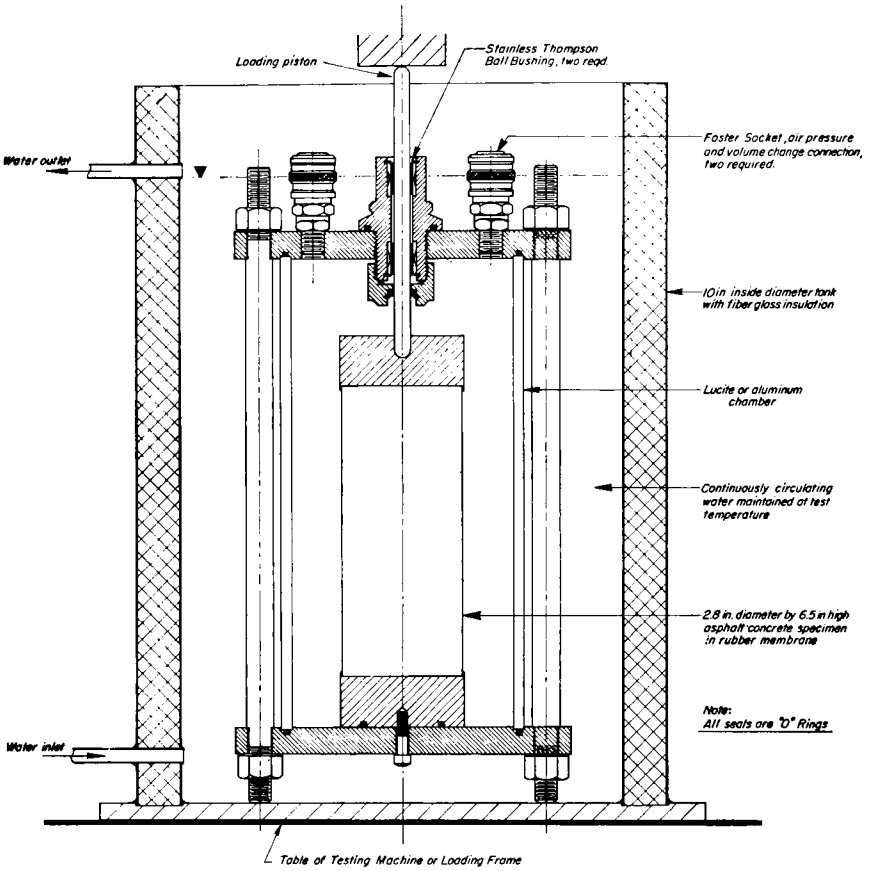

Figure 4. Triaxial cell in constant-temperature water bath for testing asphalt concrete specimens.

F could be obtained by circulating water from a control unit through the bath.

Not shown is a device attached to the triaxial cell for measuring volumetric changes in the specimens during testing. This attachment consisted of a piece of high-pressure plastic tubing clamped to a calibrated scale. For a particular test, the tubing was mounted vertically in a position somewhat above the cell and connected to it through one of the fittings in the top. The cell was completely filled with water, excluding all trapped air; the plastic tube was also filled with water to a convenient level to permit a reading to be obtained on the calibrated scale. Lateral pressure for a particular test was applied at the upper end of the plastic tubing and transmitted in turn to the test chamber. After the water in the cell and in the tubing had reached the equilibrium temperature of the bath and the specimen, a particular test was performed.

Changes in the volume of the specimen were noted on the calibrated scale. With this apparatus, volume changes as small as 0.001 cc could be recorded. Volume change meas-

urements could be observed in conjunction with the four types of test performed.

Constant-Rate-of-Strain Tests

The constant-rate-of-strain triaxial compression tests were performed at a rate of 0.10 in. per min in a universal testing machine. Load *vs* deformation characteristics for each specimen were obtained by means of a load-deformation recorder attached to the testing machine.

Relaxation Tests

Stress relaxation tests were also performed in the universal testing machine, although the hydraulic loading system of the machine was not employed. A specific value of deformation was applied to a specimen very rapidly by means of a screw jack attached to the crosshead of the testing machine; the deformation was then maintained constant during the remainder of the test. A recording of the load *vs* time characteristics of each specimen was obtained by modifying the deformation mechanism of the recorder on the testing machine to move at a constant rate.

Creep and Repeated-Load Tests

Creep and repeated-load tests were performed with the aid of pneumatically operated and electronically controlled cells mounted on a steel frame. This equipment has been described in detail elsewhere (*11*). For the creep tests, a specific magnitude of stress was applied to a specimen and maintained; readings of deformation *vs* time were observed by means of a 0.0001-in. dial gage attached to the piston of the triaxial cell. For the repeated load tests, the desired stress was applied for 1 sec at the rate of 20 applications per minute. Readings of deformation *vs* number of stress applications were also observed with a 0.0001-in. dial gage.

DEVIATORIC STRESS AND STRAIN

The major variables influencing the results of triaxial compression tests over a wide range of loading conditions are temperature, time (rate of loading), and lateral pressure, if specimen composition and preparation are held constant. The methods of viscoelasticity can be applied to the analysis of the time variable, as shown in a subsequent section; however, the concept of deviatoric stress and strain suggests that it might be used to simplify triaxial compression test results by eliminating the effects of lateral pressure.

Although the relationships involving deviatoric stress and strain are not new, and have been described in a number of publications (*1, 15, 16*), it seems appropriate to describe them briefly here. Essentially, the theory suggests that any strain in an ideal, isotropic, elastic material can be separated into two components: a change in volume with constant shape and a change in shape at constant volume. If the bulk modulus and the shear modulus are used as physical constants to represent elastic properties, a mathematical separation of pressure-volume effects and shear effects can be obtained. Because stresses and strains can be represented by tensors, they can readily be resolved into the sum of a mean normal tensor and a deviatoric tensor, which distinguish the pure pressure-volume effects from the pure shear effects.

The stress tensor can be represented by σ_{ij}, which refers to the array:

$$\sigma_{ij} = \begin{vmatrix} \sigma_{11} & \sigma_{12} & \sigma_{13} \\ \sigma_{21} & \sigma_{22} & \sigma_{23} \\ \sigma_{31} & \sigma_{32} & \sigma_{33} \end{vmatrix} \quad (1)$$

In this array σ_{11}, σ_{22}, and σ_{33} are normal components, and σ_{12}, σ_{13}, etc., are shear components. A value for

"mean normal stress" (σ) can be expressed as:

$$\sigma = \frac{\sigma_{11} + \sigma_{22} + \sigma_{33}}{3} \tag{2}$$

The mean normal stress might be thought of as a hydrostatic pressure, which can be subtracted from the stress tensor as follows:

$$S_{ij} = \begin{vmatrix} \sigma_{11} - \sigma & \sigma_{12} & \sigma_{13} \\ \sigma_{21} & \sigma_{22} - \sigma & \sigma_{23} \\ \sigma_{31} & \sigma_{32} & \sigma_{33} - \sigma \end{vmatrix} = \begin{vmatrix} S_{11} & S_{12} & S_{13} \\ S_{21} & S_{22} & S_{23} \\ S_{31} & S_{32} & S_{33} \end{vmatrix} \tag{3}$$

The array S_{ij} is called the "deviatoric stress tensor." Consideration of these relationships shows that the stress represented by Eq. 2 tends to alter the volume of the material, whereas the stress represented by Eq. 3 tends to alter its shape.

In similar fashion, it is possible to separate the strain tensor ϵ_{ij} into a mean normal strain ϵ plus a deviatoric strain tensor (e_{ij}), with

$$\epsilon = \frac{\epsilon_{11} + \epsilon_{22} + \epsilon_{33}}{3} \tag{4}$$

and

$$e_{ij} = \begin{vmatrix} \epsilon_{11} - \epsilon & \epsilon_{12} & \epsilon_{13} \\ \epsilon_{21} & \epsilon_{22} - \epsilon & \epsilon_{23} \\ \epsilon_{31} & \epsilon_{32} & \epsilon_{33} - \epsilon \end{vmatrix} \tag{5}$$

Inspection of these two relationships shows that the strain represented by Eq. 4 is a measure of the volumetric change of the material and the strain represented by Eq. 5 is a measure of its shape distortion.

These expressions can be used to establish a relationship between stress and strain. If the bulk modulus, B, governs volumetric behavior, the following expression is valid:

$$\sigma = 3B\epsilon \tag{6}$$

The shape deformation is determined by the shear modulus G, which relates the deviatoric stress tensor term by term to the deviatoric strain tensor:

$$S_{11} = 2Ge_{11} \qquad S_{12} = 2Ge_{12} \qquad S_{13} = 2Ge_{13}$$
$$S_{21} = 2Ge_{21} \qquad \text{etc.} \tag{7}$$

The first term of the last array (Eq. 7) is of special interest in the present discussion:

$$S_{11} = 2Ge_{11} \tag{8}$$

This is an expression which relates axial stress and strain after a correction for lateral pressure. Theoretically, such a relation should produce—in the case of triaxial tests performed on asphaltic paving materials at a given temperature and load rate—stress-strain curves of identical nature, regardless of lateral pressure.

To evaluate this hypothesis, a series of constant-rate-of-strain tests were performed at three temperatures, 40 F, 77 F, and 140 F, and at a single strain rate, 0.10 in. per min. At each temperature, results were obtained for three lateral pressures, 0 (unconfined), 43.8 psi (3 atmospheres) and 250 psi. During each test, measurements of volume change were recorded to permit the computation of deviatoric strains.

The results of each test were prepared as shown in Figure 5. There is a difference between deviatoric stress and the so called deviator stress which is commonly reported for the results of triaxial tests

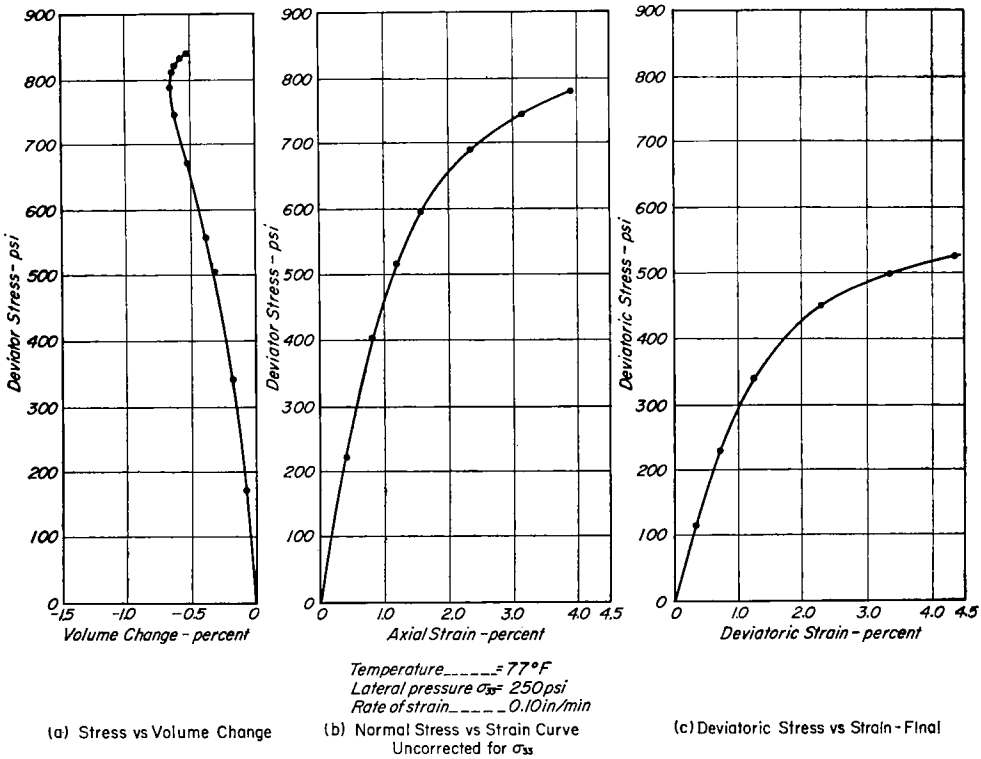

Figure 5. Data required to develop deviatoric stress *vs* strain curves.

on both asphalt paving materials and soils and which is simply $(\sigma_{11}-\sigma_{33})$. Actually the deviator stress and the deviatoric stress are related as follows:

$$S_{11}=\frac{2}{3}(\sigma_{11}-\sigma_{33}) \qquad (9)$$

Figure 5a shows the general type of volume change data obtained in performing the constant-rate-of-strain tests used to evaluate the deviatoric stress-strain concept. Figure 5b is a plot of the deviator stress *vs* axial strain characteristics of the same specimen. These two sets of data were combined to produce the final result given in Figure 5c, which is the desired graph of deviatoric stress *vs* deviatoric strain. Deviatoric stress was determined from the test data using Eq. 9, and deviatoric strain was determined from:

$$e_{11}=\epsilon_{11}-\epsilon \qquad (10)$$

where ϵ_{11} is the axial strain and ϵ is obtained by dividing the volume change data by three (see Eq. 4).

Figures 6, 7, and 8 are plots of data similar to that of Figure 5c. Each shows the effect of lateral pressure on constant-rate-of-strain (0.10 in. per min) tests performed at a given temperature. Although the data have been reduced to yield deviatoric relationships, there is a residual effect of lateral pressure. The phenomenon is greatest for tests at 140 F, as might be expected. At such an elevated temperature the asphalt affords little confinement to the ag-

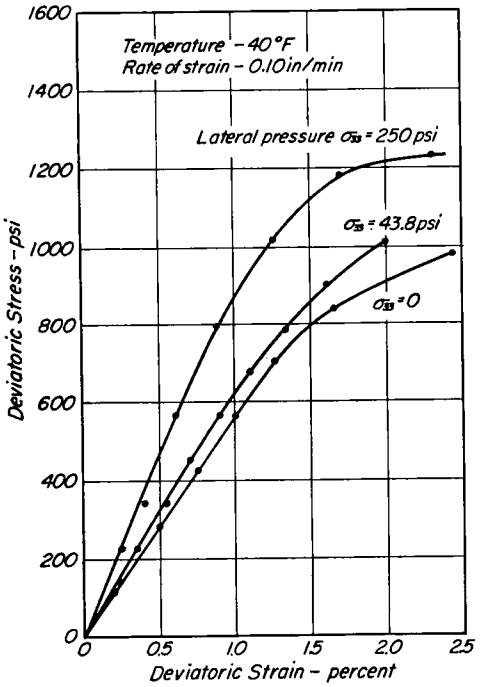

Figure 6. Comparison of results of constant-rate-of-strain tests at various lateral pressures, 40 F.

gregate, and an application of lateral pressure could be expected to produce a pronounced stiffening effect. At 40 F, where the asphalt exerts a significant confining effect, the lateral pressure still accounts for a marked deviation in the test results.

From these and other data, it has been concluded that the application of the theory of deviatoric stresses and strains to triaxial compression tests on asphalt mixtures is unwarranted, at least in connection with the use of viscoelastic model laws. Inasmuch as the theory fails to account completely for the effect of lateral pressure on such specimens, there appears little to be gained from the additional effort required for its use. Therefore, the following discussion of the use of viscoelastic models to express the stress-strain-time characteristics of asphalt mixtures deals with deviator stress and axial strain. Lateral pressure is retained as an additional variable.

VISCOELASTIC BEHAVIOR OF ASPHALT CONCRETE

The application of viscoelastic theory is by no means new in the field of asphalt paving technology, as has already been discussed. The entire process can be readily visualized by noting the three-dimensional analogy shown in Figure 9, in which each of the three basic tests—that is, the creep test, the relaxation test, and the constant-rate-of-strain test (and recognizing that the repeated-load test is a creep test carried out on a repetitive basis)—is shown schematically in relation to stress, strain and time. Viscoelastic laws simply afford a convenient method for coordinating these parameters mathematically.

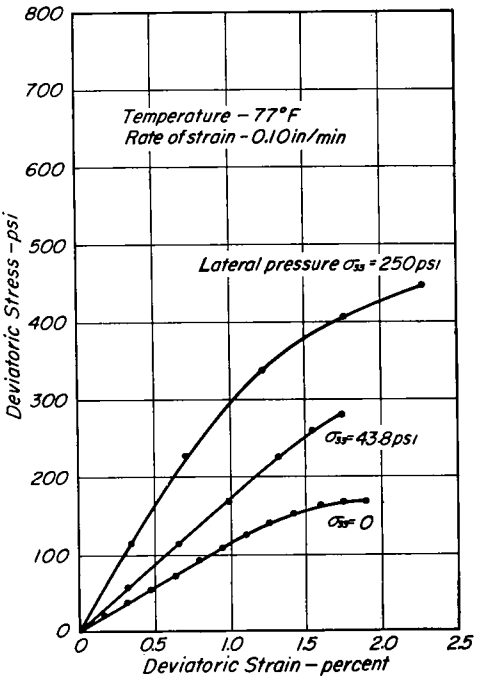

Figure 7. Comparison of results of constant-rate-of-strain tests at various lateral pressures, 77 F.

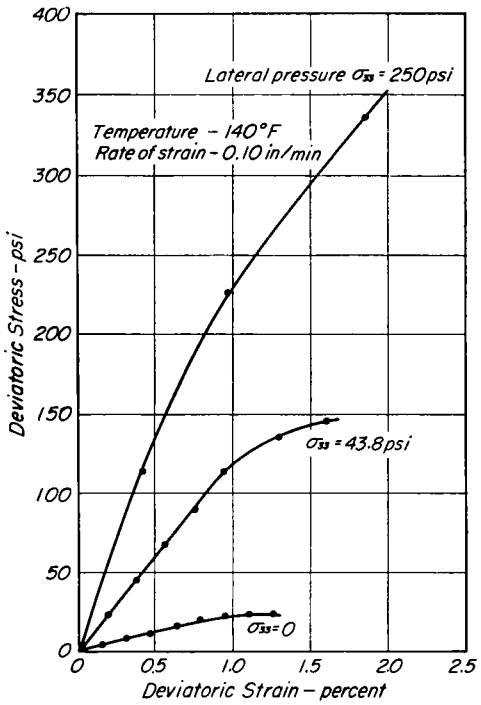

Figure 8. Comparison of results of constant-rate-of-strain tests at various lateral pressures, 140 F.

Essentially, viscoelastic models are composed of two basic elements—purely elastic springs and purely viscous dashpots. These elements are combined into various parallel and series configurations to produce mathematical expressions for stress-strain-time relations which may suit a given material under study. The most familiar models are the Voight or Kelvin (Fig. 10a) and the Maxwell (Fig. 10b). By the application of Hooke's law and Newton's law relating to viscous flow, the basic differential equation governing the behavior of the Voight model can be shown to be

$$\sigma(t) = E\,\epsilon(t) + \eta\,\frac{d\epsilon(t)}{dt} \qquad (11)$$

The differential equation for the Maxwell model is

$$\frac{d\epsilon(t)}{dt} = \frac{1}{\eta}\sigma(t) + \frac{1}{E}\,\frac{d\sigma(t)}{dt} \qquad (12)$$

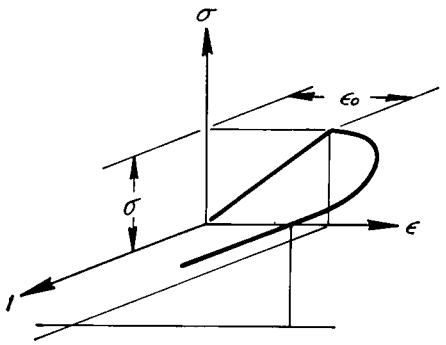

(a) Creep Test

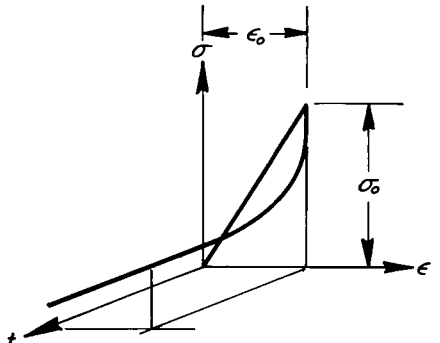

(b) Relaxation Test

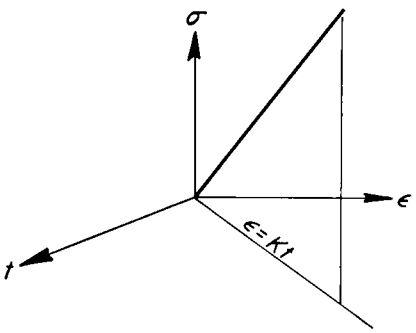

(c) Constant-Rate-of-Strain Test

Figure 9. Stress-strain-time relationships for triaxial compression tests.

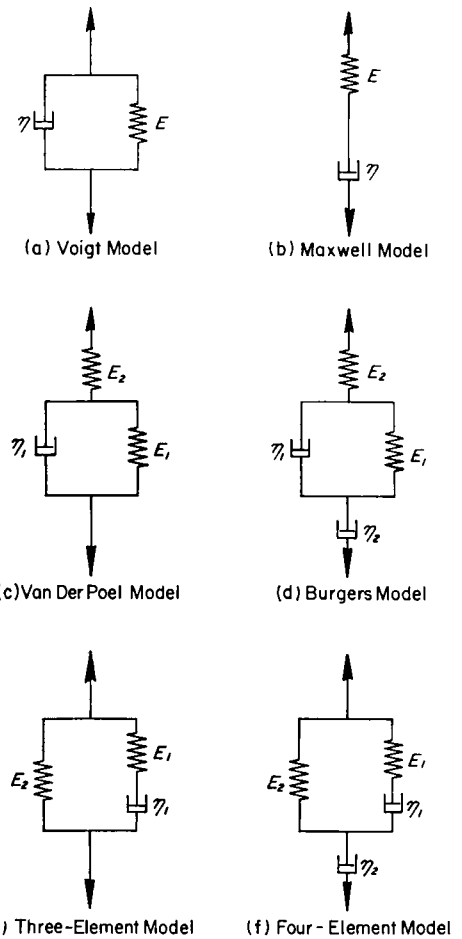

Figure 10. Viscoelastic models.

Unfortunately, neither of these simple models is sufficient to describe the behavior of a material such as asphalt concrete. To obtain representative behavior of most materials it is necessary to add more elements to the model system. When this is done, however, the mathematical operations required to define behavior become quite complex. Familiar configurations mentioned in connection with asphalts and asphalt mixtures are the models suggested by Van der Poel (Fig. 10c) and Burger (Fig. 10d). To better define material behavior, it may, in some instances, be necessary to couple a finite or infinite number of Voight or Maxwell elements. It has been suggested, for example, that stress relaxation results on asphalt concrete can be approximated closely by a model composed of an infinite number of Maxwell units in parallel (*8*).

In actuality, the ideal model for an investigation such as this is one of the utmost simplicity consistent with a satisfactory expression of material properties. Although the results of a given triaxial test might be simulated closely by a configuration with a finite or infinite number of elements, the application of the resulting mathematical formulations to the analysis of a flexible pavement system would prove extremely difficult. In addition, if it is desired to fit a single equation representing the stress-strain-time properties of asphalt concrete, for example, to the results of several different types of tests, it is necessary to keep that equation as simple as possible.

For the analysis presented in this paper, the viscoelastic model shown in Figure 10e was selected (with possible modification to be discussed later). This combination is capable of instantaneous elastic deformation, retarded deformation, and recovery. Its basic differential equation can be stated as:

$$\left[E_1+\eta_1\frac{d}{dt}\right]\sigma(t) = \left[E_1E_2+\eta_1(E_1+E_2)\frac{d}{dt}\right]\epsilon(t) \qquad (13)$$

For the constant-rate-of-strain test, where $\epsilon = K\,t$ and $\epsilon(0)=0$, the solution of Eq. 13 is

$$\sigma(t) = E_1\,\tau\,K\left[1-\exp\left(-\frac{t}{\tau}\right)\right]+E_2\,K\,t \qquad (14)$$

In which $\tau(=\eta_1/E_1)$ is the relaxation time of the material under static loading.

For the relaxation test, where $\epsilon = \epsilon_0$ (const) and $\sigma_0 = \epsilon_0(E_1+E_2)$, the solution of Eq. 13 is

$$\sigma(t) = \epsilon_0 E_1 \exp\left(-\frac{t}{\tau}\right) + E_2 \epsilon_0 \qquad (15)$$

For the creep test, the solution of Eq. 13 may best be given in four parts (*8*), as follows (see Fig. 11):

1. Segment *ab*, instantaneous elastic response at $t=0$, with

$$\epsilon(0) = \frac{\sigma}{E_1+E_2} \qquad (16)$$

2. Segment bc, viscoelastic strain at constant stress, $0<t<t_0$, with

$$\tau^* = \eta_1\left[\frac{E_1+E_2}{E_1E_2}\right]$$

(the bracketed expression is the elastic compliance of the two springs).

$$\epsilon(t) = \sigma\left[-\frac{E_1}{E_2(E_1+E_2)}\exp\left(-\frac{t}{\tau^*}\right)+\frac{1}{E_2}\right] \qquad (17)$$

3. Segment cd, instantaneous elastic response at $t=t_0$ upon unloading, with change in strain $\Delta\epsilon$, where

$$\Delta\epsilon = \frac{\sigma}{E_1+E_2} \qquad (18)$$

4. Segment de, strain recovery at zero stress, $t_0<t<t_1$, with

$$\epsilon(t) = \frac{\sigma E_1}{E_2(E_1+E_2)} \times\left[-\exp\left(-\frac{t}{\tau^*}\right)+\exp\left(-\frac{t-t_0}{\tau^*}\right)\right] \qquad (19)$$

The three-element model, if undisturbed during creep recovery, will return to zero strain. If, however, it is subjected to repeated-load applications (Fig. 11), the situation may be different. For the repeated-load test, Eqs. 16, 17, 18, and 19 still apply to the first load cycle, because it is identical to the creep loading. The same equations can be used to study the second cycle of load, as the value of strain at $t=t_1$ can be taken as the new initial value. By this same approach, the cycling may be examined indefinitely. It is important to note that, if the cycle is such that the model does not recover completely between load applications, cumulative build-up of strain can occur during the repeated-load test (*8*).

Eqs. 14 through 19 establish completely the mathematical relationships necessary for employing the three-element model in connection with the four types of tests. All that remains is the evaluation of three constants, E_1, E_2, and η_1, applicable to given test conditions. For the three-element model this is best done from the results of either a creep or a relaxation test, inasmuch as simple relationships are involved (Fig. 12).

To determine the usefulness of the equations developed for the three-element model, a typical set of data was selected from each of the four test types at a temperature of 77 F and a lateral pressure of three atmospheres (43.8 psi). This lateral pressure was selected as being representative of the degree of confinement which might be afforded asphalt concrete in an actual pavement subjected to a contact pressure of 100 psi, based on theoretical analyses of stresses in elastic systems which indicate that the radial stress may be of the order of 40 percent of the axial stress (*17*). The data are plotted in Figures 13 through 16. From the results of the creep test, the following values were approximated:

$E_1 = 2.50\times10^4$ psi,

approximated: $E_1 = 2.50\times10^4$ psi, $E_2 = 1.30\times10^4$ psi, and $\eta_1 = 9.00\times10^3$ psi-min per unit strain.

The value for η_1 was obtained by fitting the exponential term in Eq. 17 to the first portion of the creep curve, because it is believed that this

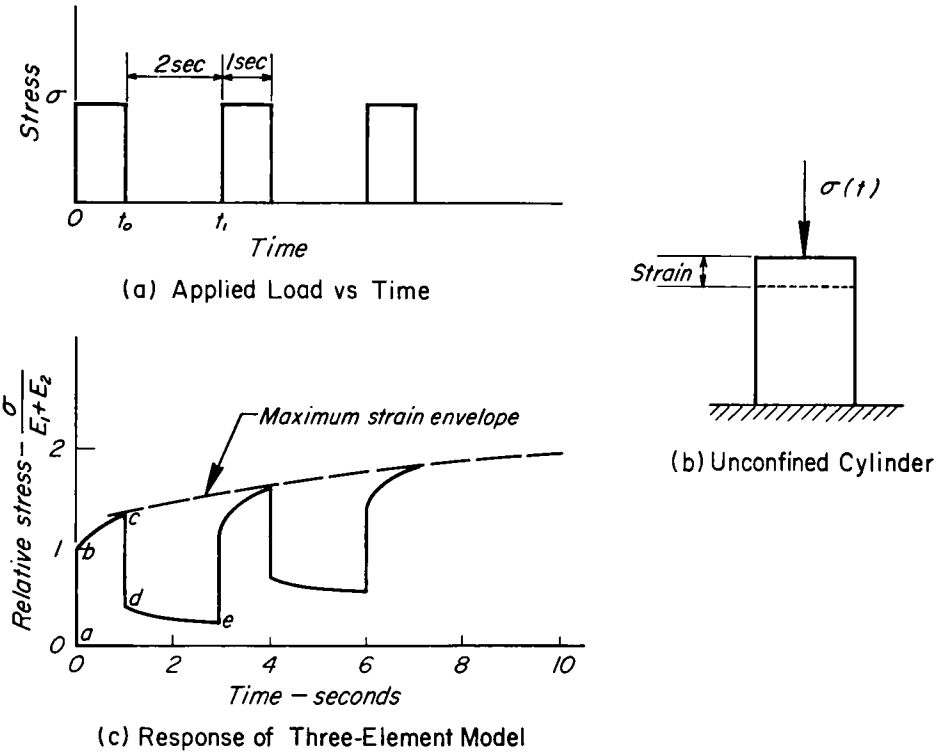

Figure 11. Creep and repeated-load relationships for the three-element model.

value might be the best for use in the other equations involved. The result was not entirely satisfactory for creep, as can be seen in Figure 13, which appears to indicate that the specimen was undergoing a constant rate of deformation with time in the latter stages of the test. This can not be explained with the three-element model. In addition, there appears to be a permanent set after creep recovery, which is also not explained by this model.

If, however, the constants obtained from the creep test are applied to Eq. 15, which represents the relaxation test, the results (Fig. 14) are in excellent agreement. Except for a small continued rate of relaxation noticeable at the end of the test, the model permits a reasonable prediction of such data from those of the creep test. The same trend is true for the constant-rate-of-strain test data shown in Figure 15; up to a strain of about 1 percent (the limit of real interest, as far as structural analysis might be concerned) the agreement between actual and predicted data is excellent.

The application of the foregoing constants to predict the results of the repeated-load test is shown in Figures 16 and 19. Figure 16 shows the first 20 cycles of testing. The apparent discrepancy between the initial measured strain and the predicted strain can be explained by the difficulties involved in measuring this initial increment (due to seating and continuity problems); otherwise, the model predicts quite well the build-up of deformation. Figure 19 shows the same repeated load test in its entirety, with the predicted curve. It should be noted that it was necessary

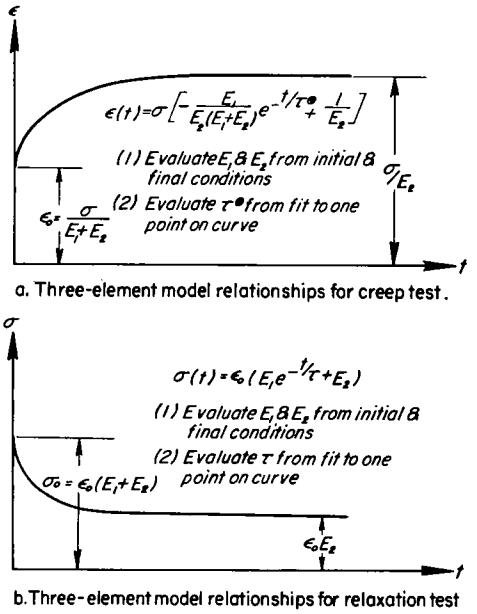

Figure 12. Determination of three-element model constants from triaxial compression test results.

to employ an electronic computer to obtain the predicted data, inasmuch as the calculation of the deformation pattern for several thousand cycles of load would have been extremely tedious and time consuming by desk calculation procedures. Figure 19 shows that the three-element model lacks the ability to account for the continual increase in strain measured in the later stages of the test. However, over a reasonably large number of cycles of stress application the model reasonably predicted the deformation pattern.

The foregoing application of the equations governing the stress-strain-time characteristics of the three-element model appears to furnish proof that viscoelastic theory has a place in the analysis of the physical behavior of asphalt concrete under load. Because the model selected was extremely simple there were certain properties (particularly in the case of the creep test) which were not explained by the theory. However, it might be true that the agreement between test and theory was sufficient to establish some grounds for the use of this model, or possibly a modified form of it, in certain types of structural analysis concerned with flexible pavements.

One possible modification to the three-element model which suggests itself immediately from an examination of the creep data in Fig. 13 is shown in Figure 10f. This configuration is formed by the simple addition of a dashpot in series with the previous model. Its basic differential equation can be stated as

$$\left[\eta_1\,\eta_2\,(E_1+E_2)\frac{d^2}{dt^2}+E_1\,E_2\,\eta_2\frac{d}{dt}\right]\epsilon(t)$$

$$=\left[\eta_1\eta_2\frac{d^2}{dt^2}+(E_1\eta_2+E_1\eta_1+E_2\eta_1)\frac{d}{dt}+E_1E_2\right]\times\sigma(t) \quad (20)$$

Solution of Eq. 20 for the four different loading conditions becomes considerably more difficult than for Eq. 13. However, the creep test equation can be obtained by superimposing the strain in the added dashpot on that of the three-element model. The equation for the strain in creep is

$$\epsilon(t)=\sigma\left[-\frac{E_1}{E_2(E_1+E_2)}\exp\left(-\frac{t}{\tau^*}\right)+\frac{1}{E_2}+\frac{t}{\eta_2}\right] \quad (21)$$

It can be seen that Eq. 21 is the same as Eq. 17, except for the last term. This term can be used to account for the continued increase in strain with time shown in Figure 13.

As was the case for the three-element model, it is possible to deal with the repeated-load test for the four-element model by repetitively

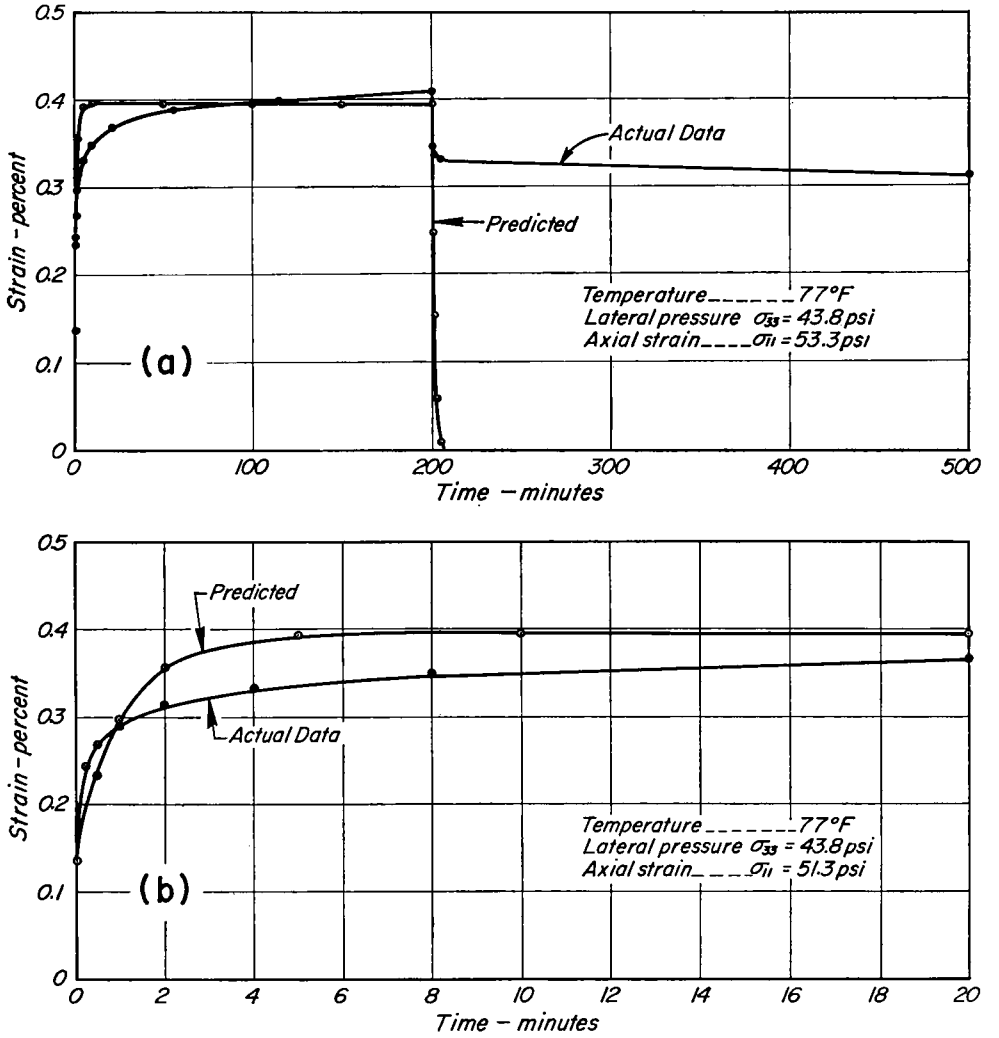

Figure 13. Comparison of creep test data and predicted data (a) using three-element model, and (b) expanded scale for first 20 min.

applying the conditions of the creep test. However, solution of Eq. 20 for either the constant-rate-of-strain test or the relaxation test is more difficult. To illustrate the complexity of these operations, the solution for the relaxation test is as follows:

$$\sigma(t) = \frac{\epsilon_0}{R_2 - R_1}[(C_3 R_2 - C_4)\exp(-R_2 t) + (C_4 - C_3 R_1)\exp(-R_1 t)] \quad (22)$$

in which

$$C_1 = \frac{E_1}{\eta_1} + \left(\frac{E_1 + E_2}{\eta_2}\right),$$

$$C_2 = \frac{E_1 E_2}{\eta_1 \eta_2}$$

$$C_3 = E_1 + E_2$$

$$C_4 = \frac{E_1 E_2}{\eta_1}$$

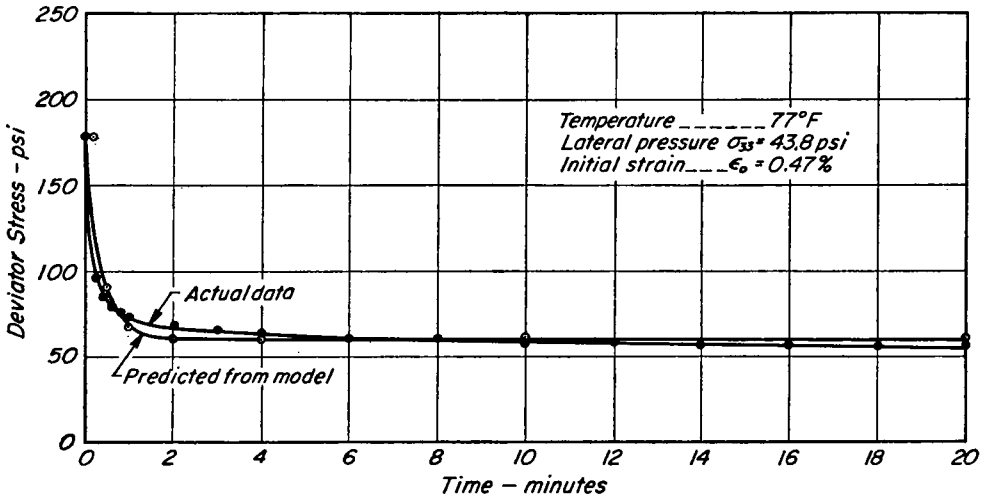

Figure 14. Comparison of relaxation test data and predicted data using three-element model.

$$R_1 = \frac{C_1}{2} + \frac{1}{2}\sqrt{C_1^2 - 4C_2},$$

$$R_2 = \frac{C_2}{2} - \frac{1}{2}\sqrt{C_1^2 - 4C_2}$$

For a comparison between the results of the three-element model and those obtained from the four-element model, suitable constants for Eq. 20 are: $E_1 = 2.45 \times 10^4$ psi, $E_2 = 1.35 \times 10^4$ psi, $\eta_1 = 8.70 \times 10^3$ psi-min per unit strain, and $\eta_2 = 3.67 \times 10^7$ psi-min per unit strain.

These values were again obtained from the results of the creep test. The resulting equation for creep is given in Figure 17, together with the curve given in Figure 13. The increase in suitability is obvious, as the extra dashpot provides for the constantly increasing strain function and also permits an allowance for permanent deformation. It should be noted, however, that the predicted permanent deformation is far too small to account for that measured during the test.

The same constants can be used in

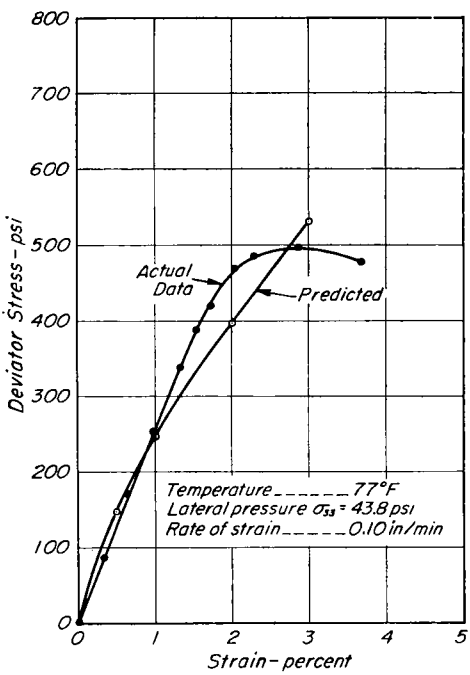

Figure 15. Comparison of constant-rate-of-strain test data and predicted data using three-element model.

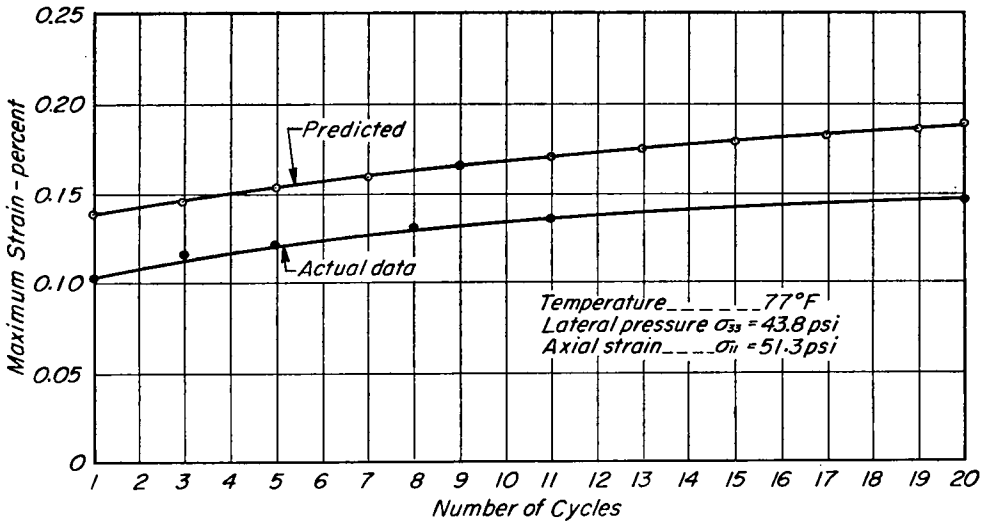

Figure 16. Comparison of repeated-load test data and predicted data using three-element model.

Eq. 22 to predict the results of the relaxation test previously plotted in Figure 14. Figure 18 compares the predicted values from Eq. 22 with these data. Reasonably good agreement is obtained, and the added dashpot provides an allowance for the slow decrease of stress with time indicated at the end of the test period.

The prediction of repeated-load test results can be accomplished for the four-element model by first computing the deformation due to the three-element portion of the configuration (same computer program as for the original three-element model, but with different values of E_1, E_2 and η_1). To this deformation is added the straightline deformation with time which is the result of loads applied to the added dashpot represented by η_2. The results of this computation are shown in Fig. 19 using the previously given values for E_1, E_2, η_1 and η_2. The agreement between the actual and predicted data is good for the early stages of the test, as was the case for the three-element model. However, with increased number of stress applications considerable deviation of the results is apparent. This discrepancy is probably due to a change in specimen properties with progressive deformation. Mack (*5*) has illustrated similar stress history effects. For the particular specimen under investigation it is possible that η_2 would increase as the specimen densified under load. Although such conditions could be handled by much more complicated models, they are beyond the scope of the work presented here.

From the foregoing discussion it can be seen that a comparison of the three-element model with the four-element model seems strongly in favor of the latter unit. However, the increased computational difficulty associated with the four-element model may practically preclude its use in the structural analysis of flexible pavements.

The foregoing discussion has presented some examples of the usefulness of viscoelastic theory in dealing with the stress-strain-time characteristics of asphalt concrete. There seems little doubt that such theory can be of value in developing more

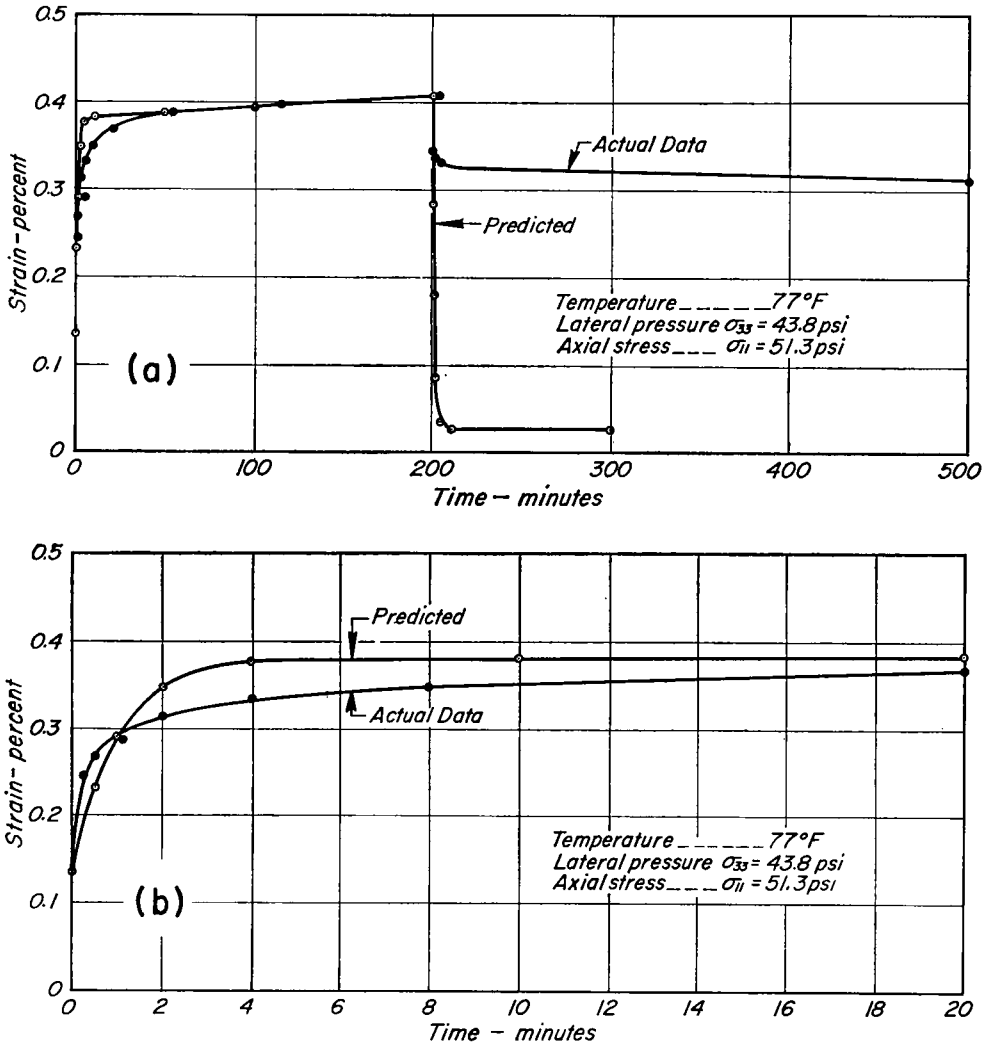

Figure 17. Comparison of creep test data and predicted data (a) using four-element model, and (b) expanded scale for first 20 min.

insight into the fundamental behavior of asphalt concrete, particularly in understanding the effects of such variables as type of asphalt, asphalt content, aggregate type and gradation, temperature, and confining pressure. Moreover this approach may also prove to be useful in the analysis of flexible pavements because the time variable can be considered. However, before this approach can be fully utilized considerably more research is required, not only with respect to the asphalt concrete and the effect of the variables previously cited, but also for the other materials comprising the pavement cross-section.

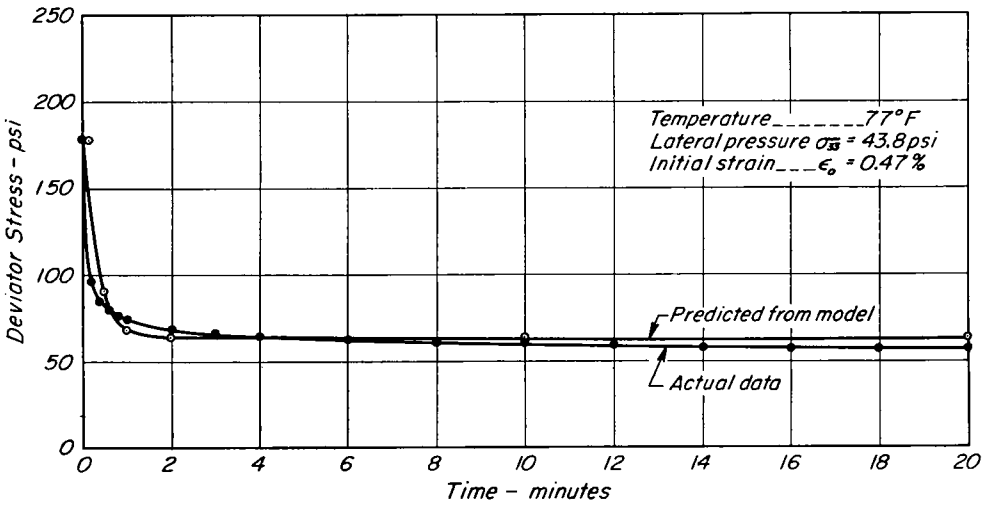

Figure 18. Comparison of relaxation test data and predicted data using four-element model.

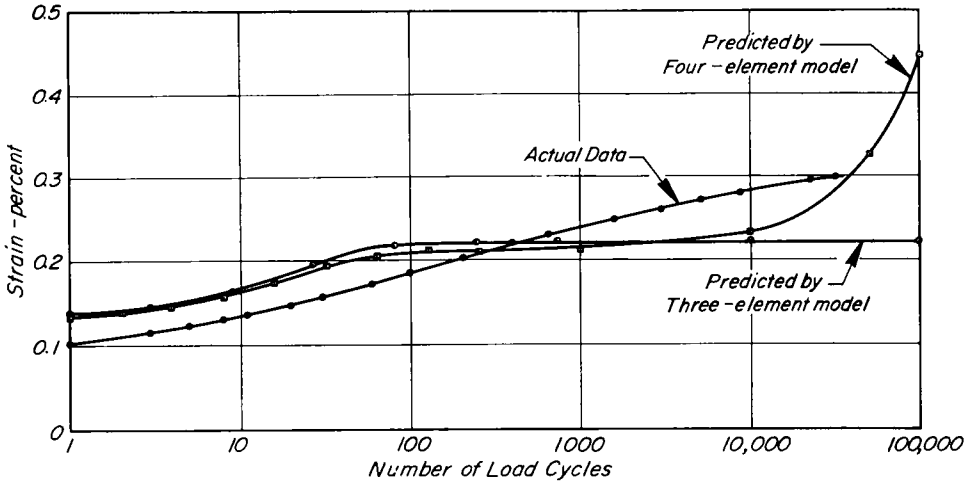

Figure 19. Comparison of actual repeated-load data with that predicted by model theory.

SUMMARY

In this paper some of the possibilities of and limitations on the use of viscoelastic principles to relate the stress-strain-time properties of asphalt concrete have been discussed in the light of the results of triaxial compression tests. The concept of deviatoric stress and strain, as it might be used to evaluate the effect of lateral pressure on these properties has been investigated; actual test data are presented to show that this consideration may not be valid for asphalt concrete, due to the large effect of confining pressures. The use of two mathematical models with the data obtained from four types of triaxial compression tests is shown, together with a comparison of values predicted from viscoelastic theory and those obtained in the laboratory.

In general, considerable evidence is presented to support the value of this form of analysis in its possible application to the structural analysis of flexible pavements.

ACKNOWLEDGMENTS

The authors would like to acknowledge the work of Russell Westmann, who aided greatly in the derivation of some of the formulas presented, and the assistance of George Dierking, who prepared the figures.

REFERENCES

1. SCHIFFMAN, R. L., "The Use of Visco-Elastic Stress-Strain Laws in Soil Testing." STP No. 254, ASTM (1959).
2. VAN DER POEL, C., "A General System Describing the Visco-Elastic Properties of Bitumens and Its Relation to Routine Test Data." *Jour. Appl. Chem.*, 4:221-236 (May 1954).
3. BROWN, A. B., AND SPARKS, J. W., "Viscoelastic Properties of a Penetration Grade Paving Asphalt at Winter Temperature." *Proc. AAPT*, 27: 35-51 (1958).
4. KUHN, S. H., AND RIGDEN, P. J., "Measurement of Visco-Elastic Properties of Bitumens Under Dynamic Loading." *HRB Proc.*, 38:431-463 (1959).
5. MACK, C., "Deformation Mechanism and Bearing Strength of Bituminous Pavements." *HRB Proc.*, 33:138-166 (1954).
6. MACK, C., "Bearing Strength Determination on Bituminous Pavements by the Methods of Constant Rate of Loading on Deformation." *HRB Proc.*, 36:221-232 (1957).
7. WOOD, L. E., AND GOETZ, W. H., "Rheological Characteristics of a Sand-Asphalt Mixture." *Proc. AAPT*, 28:211-229 (1959).
8. PISTER, K. S., AND MONISMITH, C. L., "Analysis of Viscoelastic Flexible Pavements." HRB Bull. 269, pp. 1-15 (1960).
9. MONISMITH, C. L., "On the Viscoelastic Behavior of Asphalt Concrete." To be published.
10. GRIFFIN, R. L., MILES, T. K., PENTHER, C. J., AND SIMPSON, W. C., "Sliding Plate Microviscometer for Rapid Measurement of Asphalt Viscosity in Absolute Units." In *Road and Paving Materials*, ASTM STP No. 212 (1957).
11. MONISMITH, C. L., "Flexibility Characteristics of Asphaltic Paving Mixtures." *Proc. AAPT*, 27:74-108 (1958).
12. MONISMITH, C. L., AND SECOR, K. E., "Thixotropic Characteristics of Asphaltic Paving Mixtures with Reference to Behavior in Repeated Loading." *Proc. AAPT*, Vol. 29 (1960).
13. "Standard Specifications." California Division of Highways (Aug. 1954).
14. SEED, H. B., "A Low-Cost Kneading Compactor." Information Circ. No. 27, Inst. of Transportation and Traffic Engineering, Univ. of California, Berkeley.
15. LOVE, A. E. H., "The Mathematical Theory of Elasticity." 4th ed. Cambridge University Press (1927).
16. ALFREY, T., AND GURNER, E. F., "Rheology, Theory and Application." Vol. 1, pp. 387-390. Ed. by F. R. Eirich, Academic Press, New York (1958).
17. MEHTS, M. R., AND VELETSOS, A. S., "Stress and Displacement in Layered Systems." Structural Research Series No. 178, Univ. of Illinois (June 1959).